



NASA-TM-112093

AIAA 94-0030

**Experimental Investigation of Plume-Induced
Flow Separation on the National Launch
System 1¹/₂-Stage Launch Vehicle**

A. Springer

NASA Marshall Space Flight Center, Alabama

**32nd Aerospace Sciences
Meeting & Exhibit**
January 10-13, 1994 / Reno, NV

EXPERIMENTAL INVESTIGATION OF PLUME-INDUCED FLOW SEPARATION ON THE NATIONAL LAUNCH SYSTEM 1¹/₂-STAGE LAUNCH VEHICLE

Anthony M. Springer*
NASA Marshall Space Flight Center
Huntsville, Alabama

Abstract

An experimental investigation of plume-induced flow separation on the National Launch System (NLS) 1¹/₂-stage launch vehicle was done. This investigation resulted from concerns raised about the flow separation that was encountered on the *Saturn V*. A large similarity exists between configurations and nominal trajectories. The study involved the use of solid plume simulators to simulate the base pressure encountered by the vehicle due to engine exhaust plumes at predetermined critical Mach numbers based on *Saturn V* flight plume effects. The solid plume was varied in location, resulting in a parametric study of base pressure effects on flow separation. In addition to the parametric study of arbitrary plume locations, the base pressure resulting from the nominal trajectory was tested. This analysis was accomplished through two wind tunnel tests run at NASA Marshall Space Flight Center's 14x14-Inch Trisonic Wind Tunnel during 1992. The two tests were a static stability and a pressure test each using a 0.004-scale NLS 1¹/₂-stage model. This study verified that flow separation is present at Mach 2.74 and 3.48 for predicted flight base pressures at nominal or higher levels. The flow separation at the predicted base pressure is only minor and should not be of great concern. It is not of the magnitude of the flow separation that was experienced on the *Saturn V*. If the base pressure exceeds these nominal conditions, the flow separation can drastically increase, and is of concern.

Introduction

A study was done to investigate potential plume-induced flow separation during the NLS 1¹/₂-stage launch vehicle pressure test.¹ This study was to determine if separation occurs, how far forward does the separation act? The study arose from concerns over flow separation encroaching up the vehicle, as occurred with the *Saturn V* launch vehicle during the AS-501 through AS-503 flights as shown in Fig. 1. A range of base pressures was tested, bounding the expected flight base pressure levels. This range of pressures was used to account for any variances in flight conditions from

current predictions. If the current expected flight base pressures tested result in flow separation, then it is expected for these effects to occur during actual flight. The 1¹/₂-stage model was designed for obtaining pressure distributions and their resulting distributed loads. Because of this, the exact location of incipient flow separation could not be determined but the magnitude and presence of flow separation were confirmed.

Vehicle Similarities

The Apollo *Saturn V* encountered flow separation during flights of the AS-501, AS-502, and AS-503 vehicles.^{2,3} The flow separation, that occurred on vehicle AS-502, is shown graphically in Fig. 2, which depicts the magnitude and point of flow separation at 110, 120, 130, and 140 s into flight. Comparison between the *Saturn V* vehicle stations and those of the NLS 1¹/₂-stage are shown in Fig. 3. It can be seen from these diagrams that the NLS 1¹/₂-stage configuration is relatively proportional to the *Saturn V* in external configuration. Figure 4 is a closeup comparison of the base region of both vehicles. A comparison of the base pressure ratios between the AS-501, AS-502, and AS-503 flight with that of the NLS 1¹/₂-stage is shown in Fig. 5. From these plots, it is seen that the NLS has a slightly lower base pressure ratio. This lower ratio should reduce the magnitude of flow separation, since flow separation is a function of base pressure. The vehicle base pressure is determined by a series of factors. The main factors are altitude, air density and pressure, and engine configuration, engine thrust level, and number of engines. The *Saturn V* trajectory and NLS trajectory are similar as seen in Fig. 6, which is a graph of dynamic pressure versus Mach number. Since the trajectories are so similar, their effect on base pressure will be approximately equal for each vehicle. The effect of engine thrust and base area, addition of engine shrouds, on base pressure is shown in Fig. 7, which is a graph of the two proposed thrust levels for the NLS 1¹/₂-stage vehicle, 583k and 650k, along with base areas of 597.4 ft², NO SH, or 769.9 ft², W SH, versus Mach. The effect of engine thrust level and base area on base pressure are easily seen.

On the *Saturn V*, the F-1 engine's plumes expanded with altitude, creating an adverse pressure gradient, causing the local free stream flow to separate from the vehicle. Exhaust gases were forced into the separated region from the base region of the vehicle. Flow separation was established at approximately 109 s on AS-501, 110 s on AS-502, and 116 s on the AS-503 vehicle. These times correspond to altitudes of

*Test Engineer, Member AIAA.

30.0 km, for AS-501, 29.5 km for AS-502, and 28.0 km for AS-503.³ The earlier flow separation on the AS-503 resulted from the 2° outboard engine cant which was not present on the AS-501 and AS-502 vehicles. The forward point of flow separation was determined from Airborne Lightweight Optical Tracking System (ALOTS) optical data for the AS-502 and AS-503 flights. The ALOTS data were unavailable for the AS-501 flight. The ALOTS data are shown in Fig. 8. The time of inboard engine cutoff (IECO) is also shown in Fig. 8. It is seen that IECO alters the exhaust plume shape, reducing the flow separation.

The flight evaluation of AS-501 through AS-503 concluded that boundary layer flow separation caused exhaust gases to recirculate forward along the side of the vehicle past the S-IC/S-II interstage, while an early center engine cutoff, as on AS-503, reduced the area affected by flow separation.

Facility Description

MSFC's 14×14-Inch Trisonic Wind Tunnel is an intermittent blowdown tunnel which operates by high-pressure air flowing from storage to either vacuum or atmosphere conditions. The transonic test section provides a Mach number range from 0.2 to 2.0. Mach numbers between 0.2 and 0.9 are obtained by using a controllable diffuser. The Mach range from 0.95 and 1.3 is achieved through the use of plenum suction and perforated walls. Each Mach number above 1.30 requires a specific set of two-dimensional contoured nozzle blocks.

A solid wall supersonic test section provides the entire range from 2.74 to 5.0 with one set of automatically actuated contour blocks. Air is supplied to a 6,000 ft³ storage tank at approximately -40 °F dew point and 425 psig.

The tunnel flow is established and controlled with a servoactuated gate valve. The controlled air flows through the valve diffuser into the stilling chamber and heat exchanger where the air temperature can be controlled from ambient to approximately 180 °F. The air then passes through the test section, which contains the nozzle blocks and test region. Downstream of the test section is a hydraulically controlled pitch sector that provides the capability of testing up to 20 angles-of-attack from -10° to +10° during each run. Sting offsets are available from obtaining various maximum angles-of-attack up to 90°.

The diffuser section has movable floor and ceiling panels which are the primary means of controlling the subsonic Mach numbers and permit more efficient running supersonically.

Tunnel flow is exhausted through an acoustically damped tower to atmosphere or into the vacuum field

of 42,000 ft³. The 14×14-Inch Trisonic Wind Tunnel is shown in Fig. 9.

Model Description

The 0.004-scale NLS 1¹/₂-stage vehicle model consisted of a cylindrical payload section 2.88 inches in length, 0.800 inch in diameter with a biconic nose cone (15°/25°). The interstage section (0.838 inch in length) connects the payload section to the "core stage" made up of a hydrogen tank, interstage, lox tank, and propulsion module. The reference engine shrouds were part of the basic model and were 0.682 inch in length and had a 0.252-inch base radius. The model utilized removable feedlines, which were installed during the flow separation study. The model had 233 0.032 pressure taps.

Test

The flow separation data for the NLS 1¹/₂-stage vehicle were obtained from TWT 734, a wind tunnel test run in MSFC's 14×14-Inch Trisonic Wind Tunnel facility to determine the 1¹/₂-stage vehicle pressure distributions in support of the detailed configuration definition. The flow separation study was run at Mach 2.74 and 3.48. These Mach numbers resulted from the analysis of *Saturn V* flight data. The aft part of the vehicle, the interstage to the base of the vehicle, was instrumented with pressure taps to provide local surface pressure data for this study. The base pressure was varied by moving a solid plume simulator along the sting at various distances from the vehicle base. Plume distances of 1, 2, and 3 inches from the vehicle's base were tested. Pressure data were obtained for each setup and also for the no-plume configuration. Model base pressures were measured using external tubes placed next to the base. The variation of model base pressure was used to simulate the effect of plume expansion on the base region, which increases the base pressure separating the flow, as seen in the *Saturn V* data.

Results

The model base pressures were averaged and are shown in Figs. 10 and 11, as a function of base pressure coefficient versus angle-of-attack for Mach numbers of 2.74 and 3.48, respectively. Also shown is the predicted base pressure coefficient, 0.09 for Mach 2.74 and 0.11 for Mach 3.48, from reference 3, which is based on *Saturn V* operational data.

The wind tunnel test results show that the predicted flight base pressure coefficient results in minor flow separation over the vehicle. The flow separation over the vehicle is seen in the plots of pressure coefficient versus vehicle station (Figs. 12 and 13). These plots show comparisons between the various plume locations, base pressures, and their effect on the pressure over the aft end of the vehicle. The magnitude of pressure increase can be determined from these plots.

The data with no plume simulator present show the reference pressure over the vehicle. Any increase in pressure over the base vehicle pressure is directly comparable to flow separation. The predicted base pressure corresponds to a plume location of 2.98 inches for Mach 2.74 and 2.4 inches for Mach 3.48. The distributions corresponding to the predicted base pressures are shown as an $x_{pl}=3$ at Mach 2.74 and an $x_{pl}=2.4$ at Mach 3.48.

Conclusions

An increase in base pressure increases the pressure over the lower part of the vehicle, thus separating the flow. The extent of flow separation and the starting range of this separation, increases as a function of base pressure. This is shown in Figs. 12 and 13, looking at a simulated plume location of 1 inch from the base ($x_{pl}=1$), the largest base pressure tested. The flow is separated for all conditions, at this base pressure, while the point of flow separation and magnitude of separation varies for the lower base pressures tested. For a plume location of $x_{pl}=1$ at all angles-of-attack, the flow is attached at station 3580 and is seen to separate after this point before station 4123, the next station on the vehicle for which there are data. The feedlines cause flow separation at the base of the vehicle up to nominally between station 4215 and 4250 for an $x_{pl}=3$, between station 4123 and 4215 for an $x_{pl}=2$. The phi locations without feedlines have partial separation up to station 4250 for some conditions. Feedlines are located at a phi of 0 and 180 for an alpha run or a phi of 90 and 270 for a beta run. No large change was seen in the flow separation fields due to angle-of-attack or angle-of-sideslip. Pressure levels vary with angle-of-attack/angle-of-sideslip, but the trends in the separated regions are not dramatically affected. The affect of angle-of-attack can be seen in Figs. 13, 14, and 15, which are graphs of pressure coefficient versus vehicle station for angles-of-attack of 0°, -4°, and 4°.

This study verified that flow separation is present at Mach 2.74 and 3.48 for predicted flight base

pressures at nominal or higher levels. The flow separation at the predicted base pressure is only minor and should not be of great concern. It is not of the magnitude of the flow separation that was experienced on the *Saturn V*. If the base pressure exceeds these nominal conditions, the flow separation can drastically increase and could be of concern.

References

1. Springer, Anthony M.: "Post-Test Report for TWT 734 The National Launch System (NLS) 1^{1/2}-Stage Pressure Test in the MSFC 14-Inch Trisonic Wind Tunnel." NASA MSFC ED35-127-92, September 9, 1992.
2. Krausse, S.C.: "Aerothermodynamic Flight Evaluation *Saturn V*, AS-502." The Boeing Company Space Division Launch Systems Branch, D5-15556-2, July 3, 1968.
3. Krausse, S.C.: "*Saturn V* Aerothermodynamic Flight Evaluation Summary—AS-501 Through AS-503." The Boeing Company Space Division Launch Systems Branch, D5-15796-1, June 19, 1969.
4. Pokora, Darlene C.: "Aerodynamic Data Base for the 1^{1/2}-Stage (1.5-RV10603) and the Heavy Lift Launch Vehicle (HLV-10607) Configurations for the National Launch System." NASA MSFC ED35-25-91, July 1, 1991.
5. Lowery, T.J.: "Effects of Flow Separation on Apollo *Saturn V* First Stage Aerodynamics." NASA MSFC R-AERO-AD-68-35, June 10, 1968.
6. Springer, Anthony M.: "Plume Induced Flow Separation On The National Launch System (NLS) 1^{1/2}-Stage Launch Vehicle." NASA MSFC ED34-TBD-93, 1993.

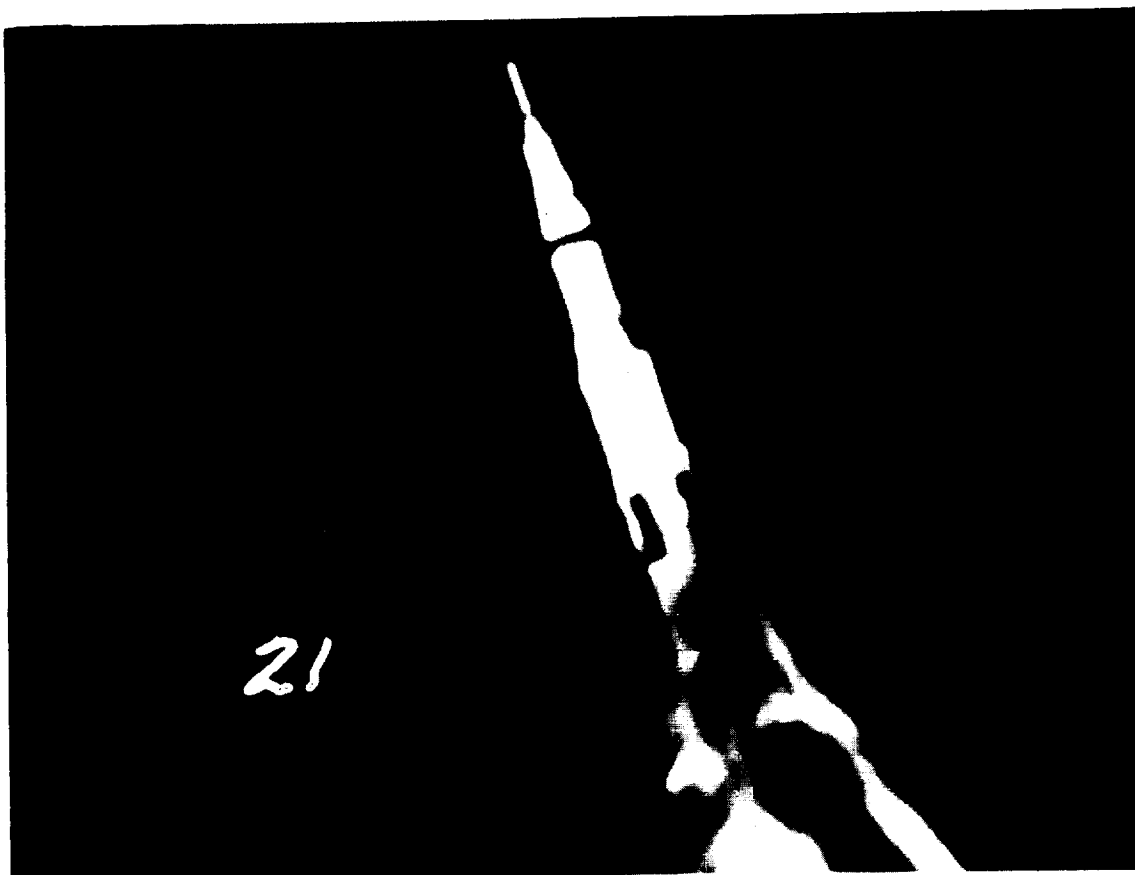


Fig. 1. Photograph of Plume-Induced Flow Separation Over the *Saturn V*, AS-502.

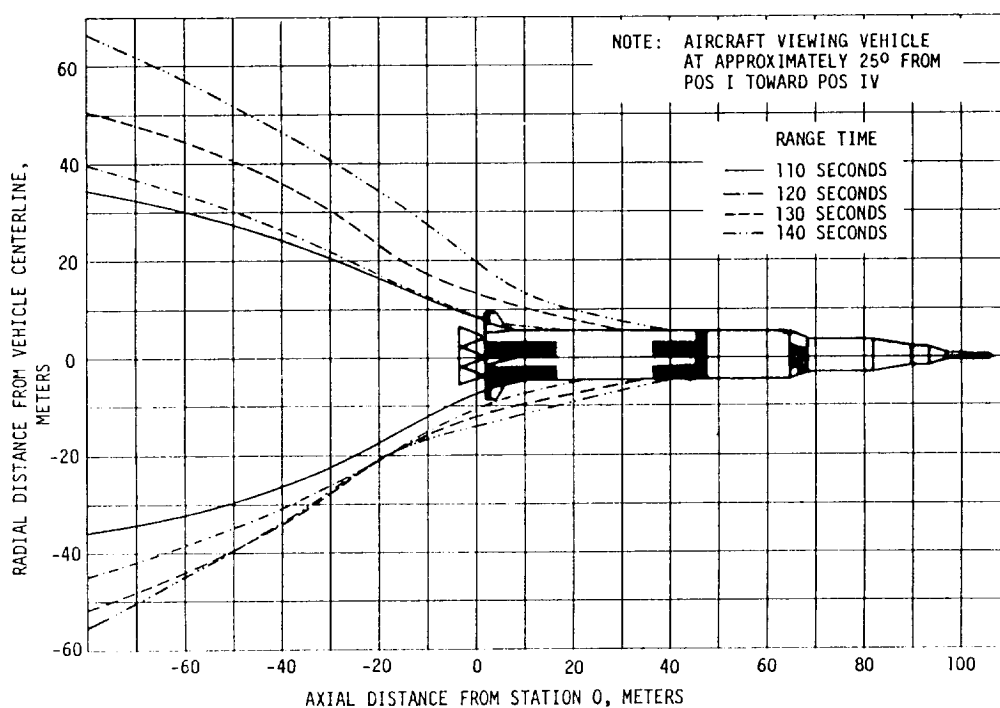
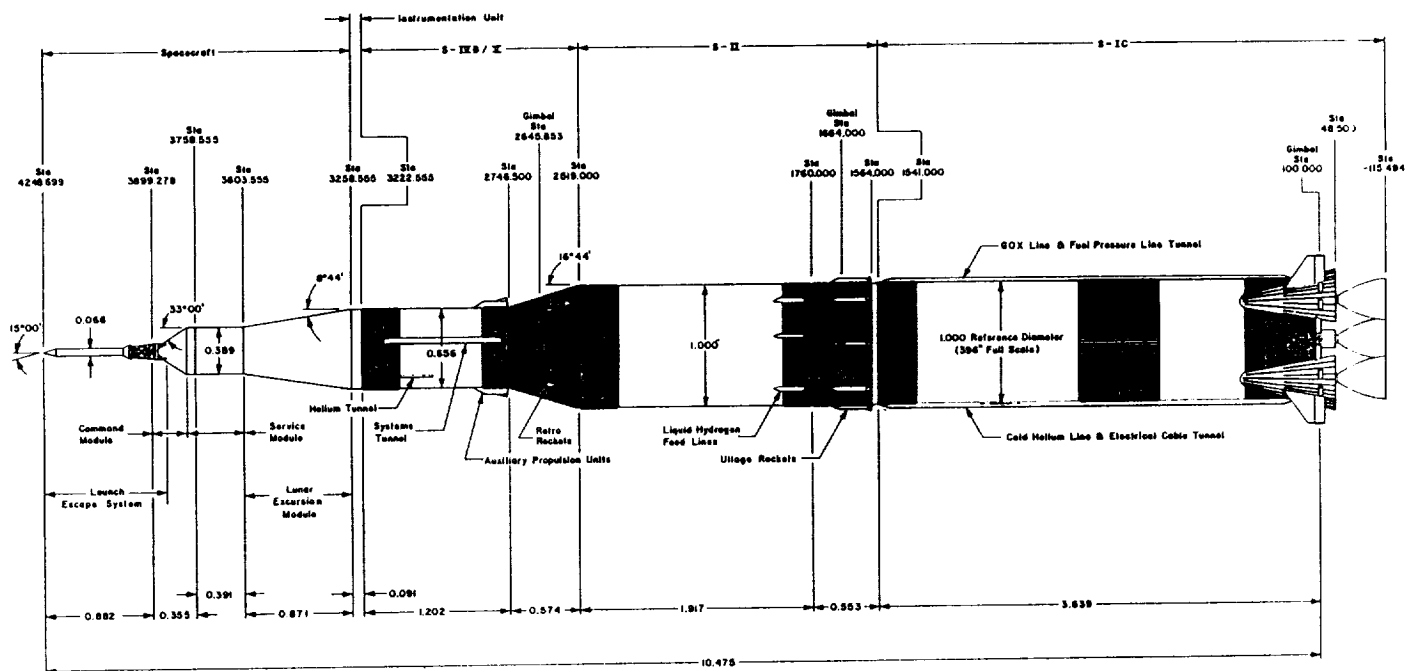


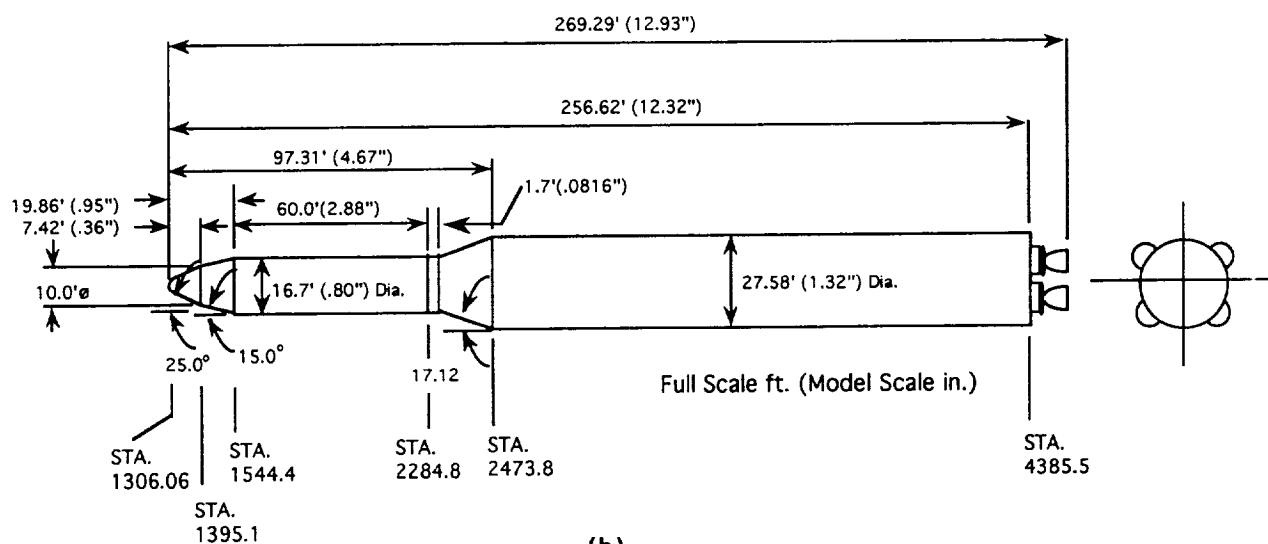
Fig. 2. Plume-Induced Flow Separation Over the *Saturn V*, AS-502.



NOTES:
 1. All vehicle stations in inches.
 2. All linear dimensions in calibers.
 3. Source: MSFC Des. DMO4106, Rev. G.

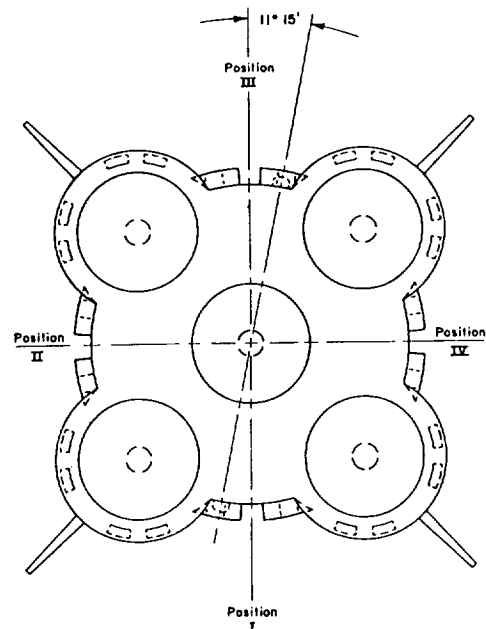
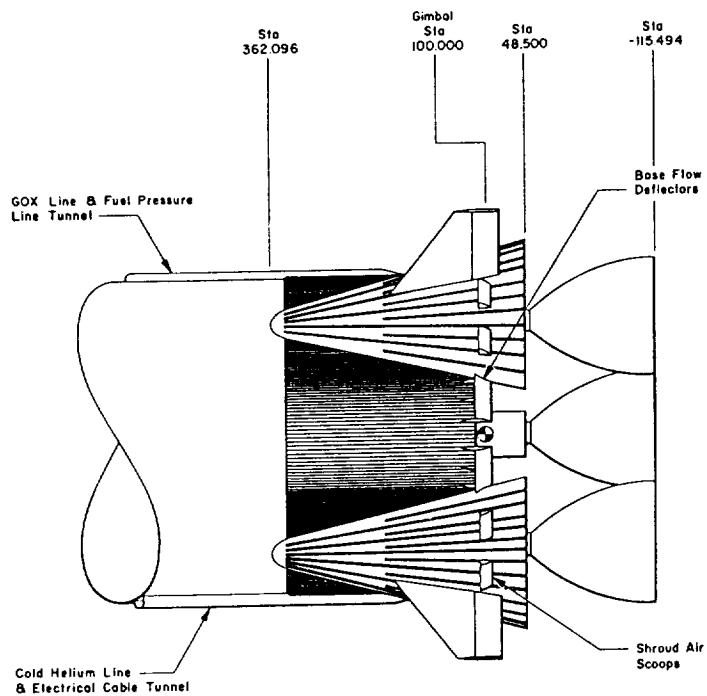
(a)

AREF=593.96 sq. ft.
 DREF=27.5 ft.

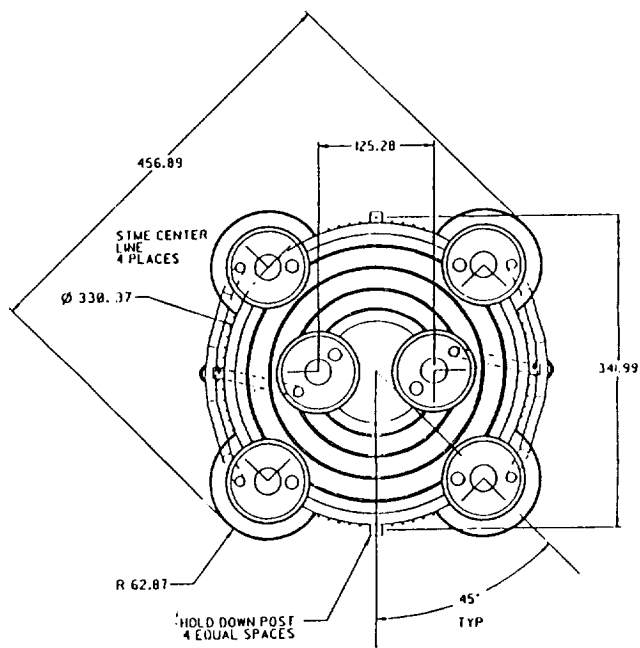
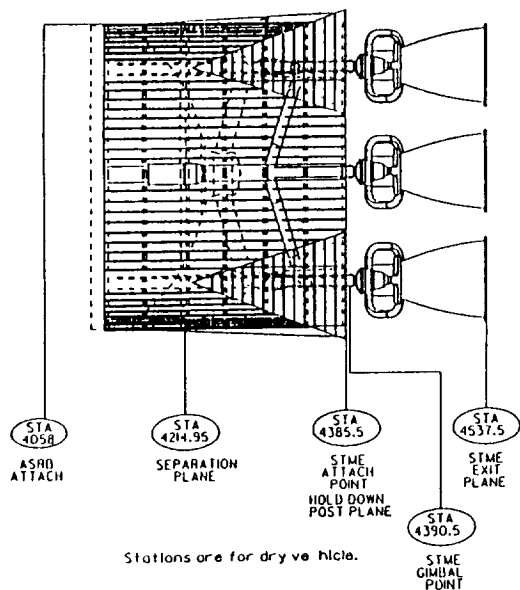


(b)

Fig. 3. Comparison of Saturn V (a) and NLS 1¹/₂-Stage (b) Geometry.



(a)



NLS 1.5 Stage Engine Arrangement

(b)

Fig. 4. Closeup of Saturn V (a) and NLS 1¹/₂-Stage (b) Base Regions.

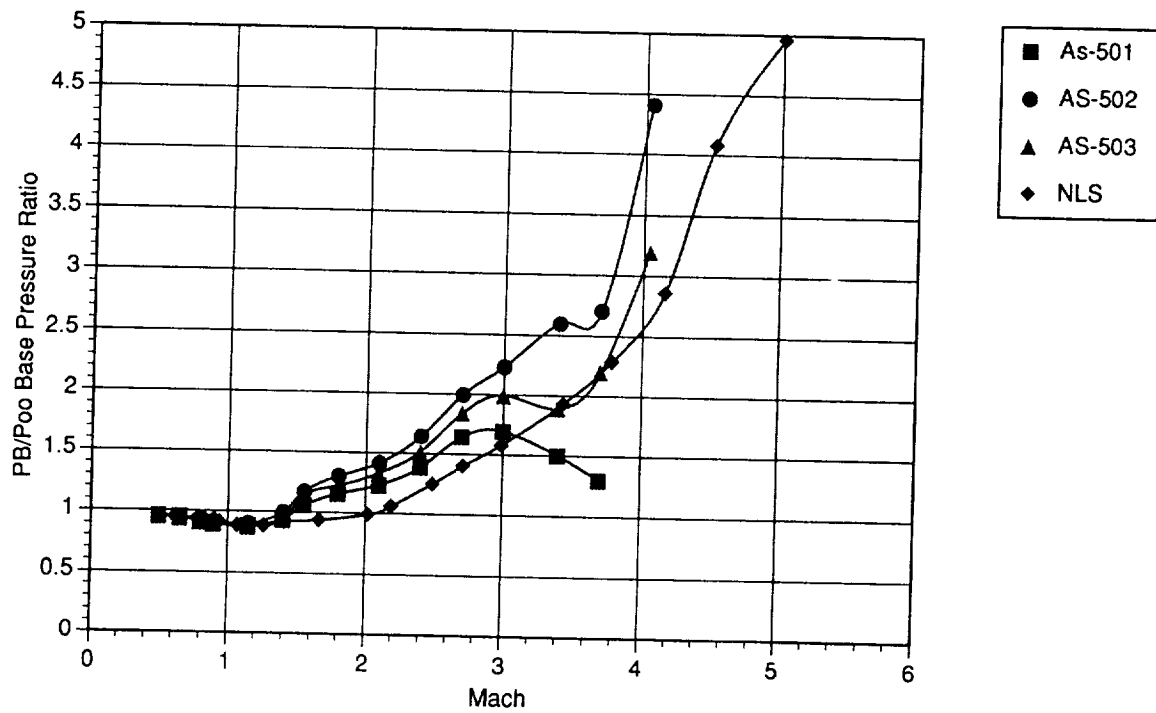


Fig. 5. Comparison of Base Pressure Ratios of *Saturn V* and NLS.

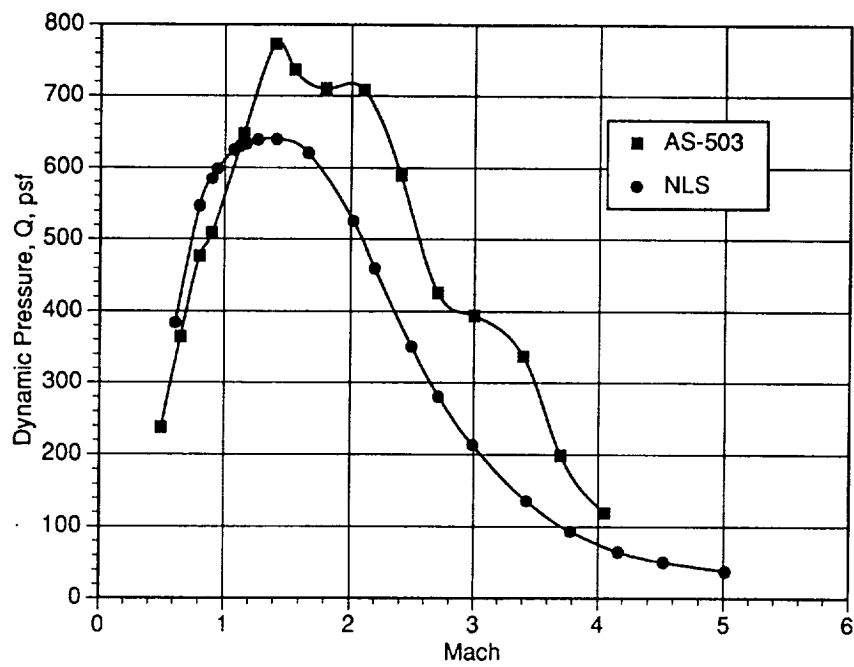


Fig. 6. Comparison of Dynamic Pressure Between *Saturn V* and NLS.

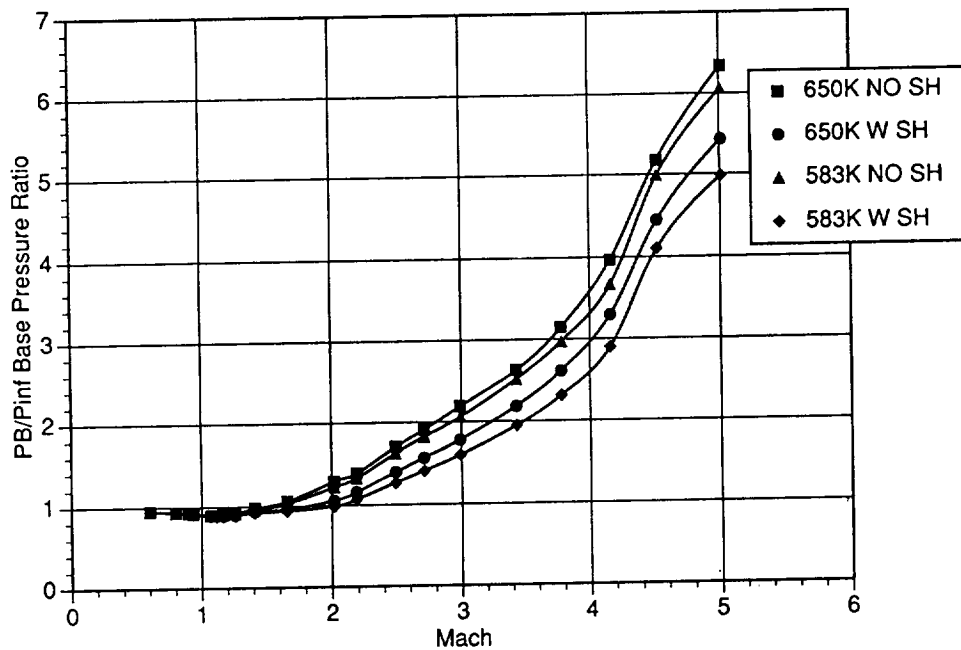


Fig. 7. Effect of Engine Thrust and Base Area on Base Pressure Ratio for the NLS 1¹/₂ Stage.

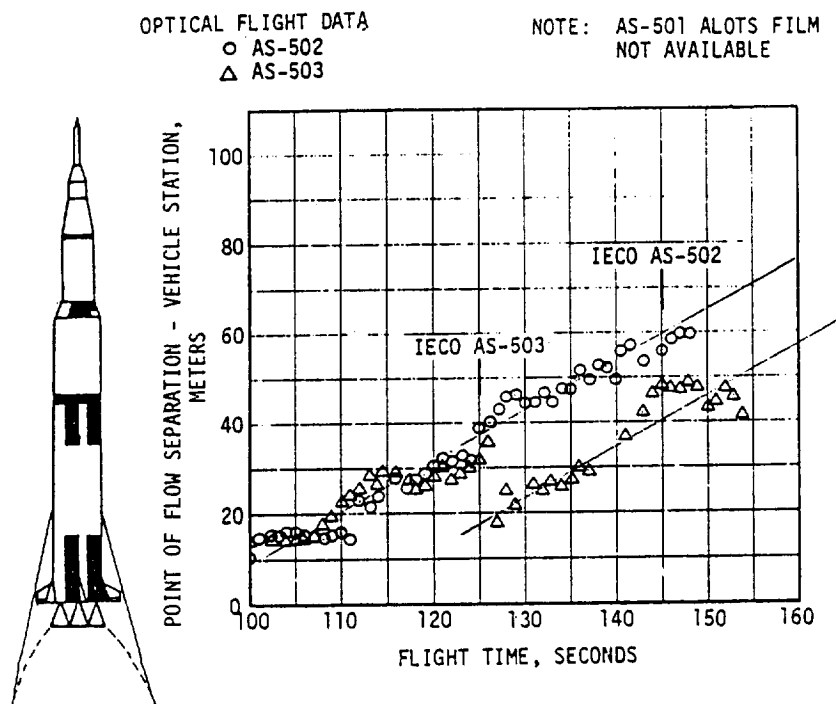


Fig. 8. Saturn V ALOTS Data.

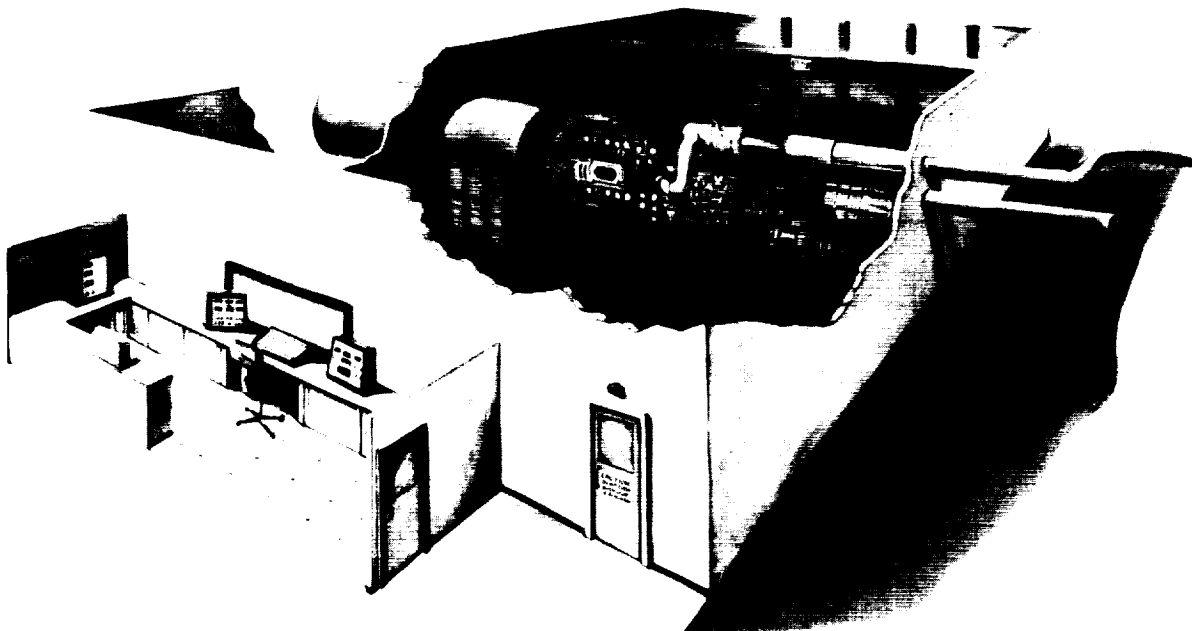


Fig. 9. The NASA MSFC 14x14-Inch Trisonic Wind Tunnel.

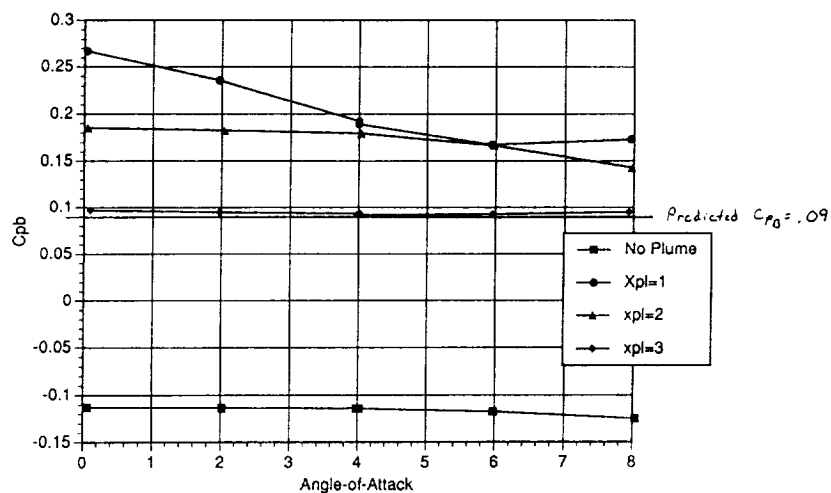


Fig. 10. Model Base Pressures at Mach 2.74.

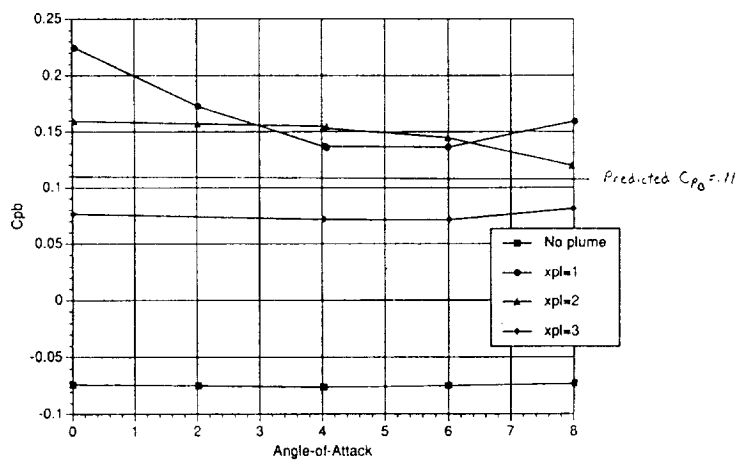


Fig. 11. Model Base Pressures at Mach 3.48.

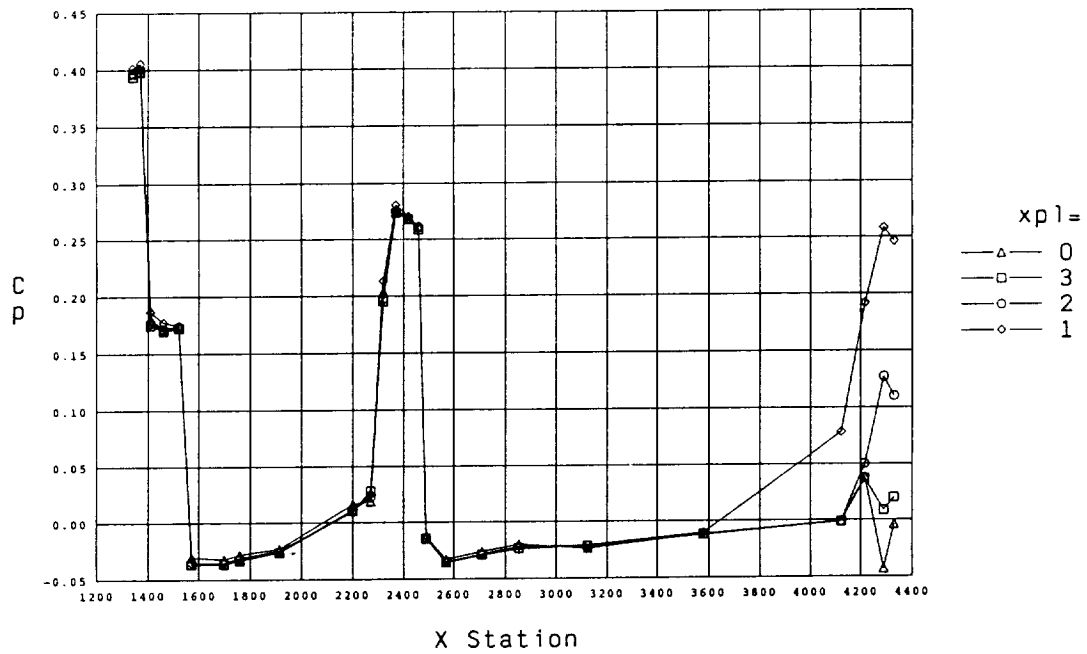


Fig. 12. Pressure Coefficient Versus Vehicle Station at Mach 2.74, $\alpha=0$, $\beta=0$, $\phi=0$.

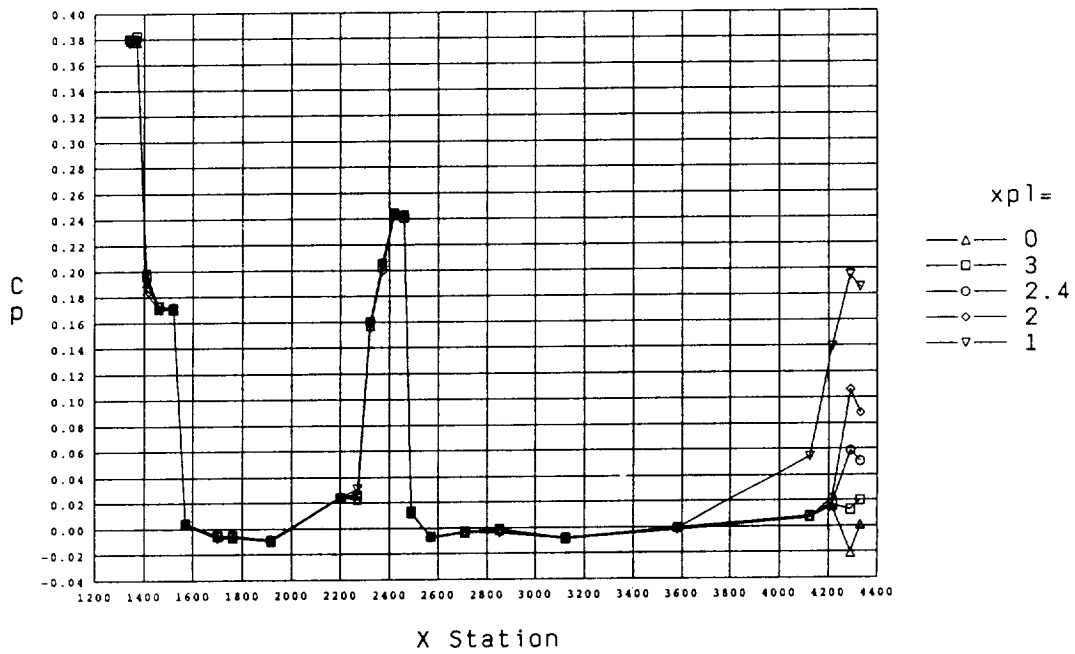


Fig. 13. Pressure Coefficient Versus Vehicle Station at Mach 3.48, $\alpha=0$, $\beta=0$, $\phi=0$.

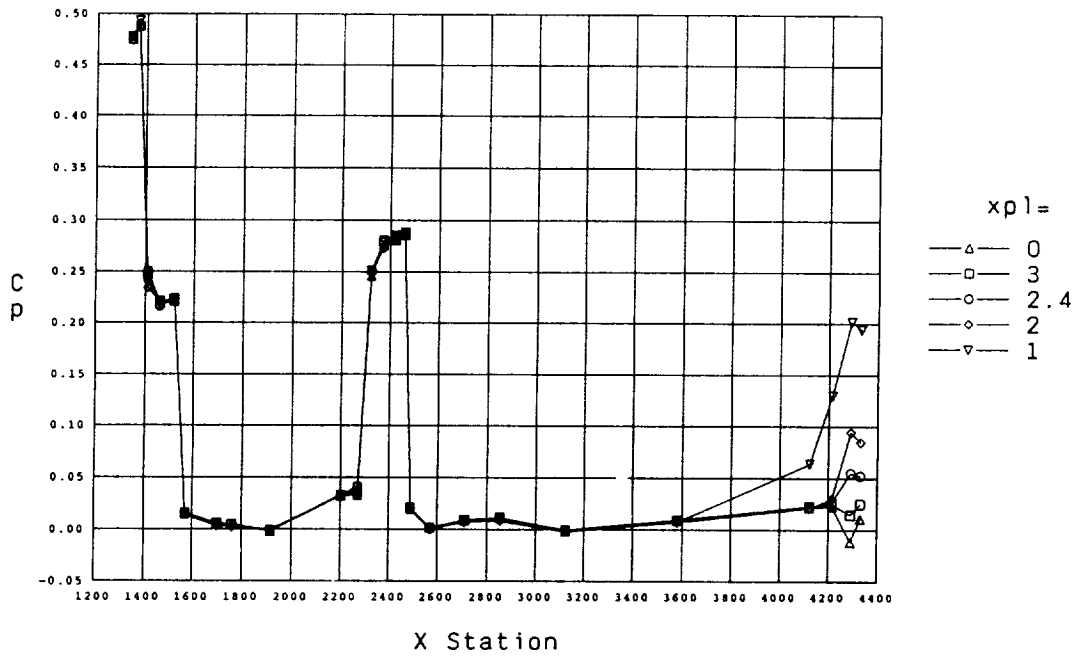


Fig. 14. Effect of Angle-of-Attack on Pressure Coefficient, Mach 3.48, $\alpha = -4$, $\beta = 0$, $\phi = 0$.

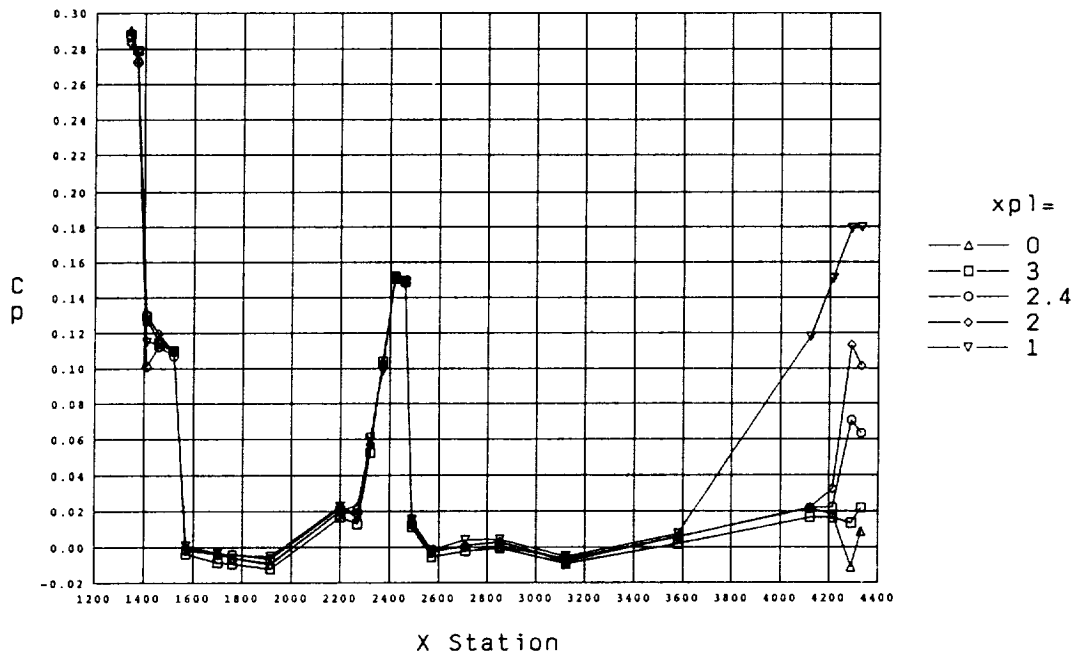


Fig. 15. Effect of Angle-of-Attack on Pressure Coefficient, Mach 3.48, $\alpha = 4$, $\beta = 0$, $\phi = 0$.